

Noise-cancelled, cavity-enhanced saturation laser spectroscopy for laser frequency stabilisation

Glenn de Vine, David E. McClelland and Malcolm B. Gray

Centre for Gravitational Physics, Faculty of Science, The Australian National University,
Canberra, ACT 0200, Australia

E-mail: glenn.devine@anu.edu.au

Abstract.

We employ a relatively simple experimental technique enabling mechanical-noise free, cavity-enhanced spectroscopic measurements of an atomic transition and its hyperfine structure. We demonstrate this technique with the 532 nm frequency doubled output from a Nd:YAG laser and an iodine vapour cell. The resulting cavity-enhanced, noise-cancelled, iodine hyperfine error signal is used as a frequency reference with which we stabilise the frequency of the 1064 nm Nd:YAG laser. Preliminary frequency stabilisation results are then presented.

1. Introduction

An atomic transition gives an absolute frequency reference which is capable of dramatically reducing laser frequency noise. As a consequence, atomic frequency references have the potential for application in space-based gravitational wave detection where very long interferometer arms with relatively large arm length differences would be sensitive to laser frequency noise coupling [1]. Atomic and molecular species which have transitions at Nd:YAG laser frequencies, such as acetylene and caesium, are typically very weak. Molecular iodine has transitions at the 532 nm doubled Nd:YAG frequency which, although still relatively weak, are stronger than those at the fundamental frequency.

Fabry-Perot interferometers provide a means of amplifying the response of weak atomic transitions [2]. However, this interferometric improvement necessarily couples laser frequency noise and mechanical noise of the interferometer into the measurement, placing stringent requirements on both the frequency noise of the interrogating laser as well as the acoustic and seismic isolation required for interferometer operation. Here we employ a new technique [3] that provides both cavity-enhanced sensitivity and noise immunity in a relatively simple experimental configuration. We use this technique to obtain a frequency reference error signal for laser frequency stabilisation.

2. A new technique: Pump-probe differencing in cavity-enhanced spectroscopy

Our technique uses a traveling-wave Fabry-Perot interferometer (FPI) which is interrogated in both directions using a pump/probe configuration (see figure 1). Both beams reflect off the cavity and are detected on respective photodetectors. The demodulated pump error signal is used to lock the ring cavity to the laser frequency [4]. In addition, the RF signals from the pump and probe are also demodulated before being subtracted from each other. By balancing

the signal amplitude of the demodulated pump relative to the demodulated probe, prior to subtraction, it is possible to cancel out the error signal resulting from cavity detuning, including mechanical FPI noise, as this is common to both.

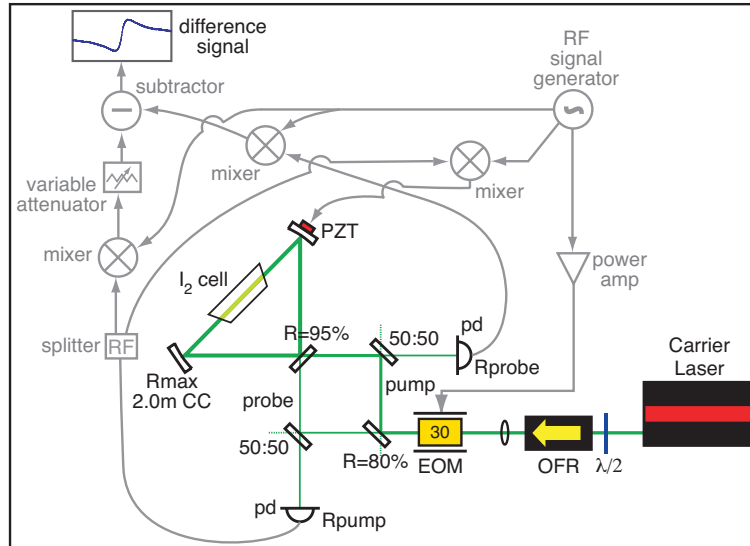


Figure 1. Schematic layout of experiment. $\lambda/2$ half waveplate; OFR optical Faraday rotator (optical isolator); EOM electro-optic modulator; pd photo-detector.

2.1. Experimental description

A simplified experimental schematic is illustrated in figure 1. Our experiment employs a three-mirror ring cavity comprised of a 5% flat input-coupler and two maximum reflectivity mirrors each with 2.00 m concave radius of curvature. Ignoring any losses, the cavity is over-coupled, with a nominal Finesse, $\mathcal{F} \approx 120$ and linewidth, FWHM (full-width at half-maximum), $\Delta\nu \approx 6.3$ MHz. The cavity geometry is that of a right-isosceles triangle with the input coupler located at the apex of the 90 degree point, with a round-trip length, $L = 0.393$ m. This gives the cavity a free spectral range, $\text{FSR} \approx 763$ MHz, an average cavity waist diameter, $\omega_{0,1} = 518.8 \mu\text{m}$ at the input coupler and an average cavity waist diameter, $\omega_{0,2} = 530.0 \mu\text{m}$ mid-way between the two curved cavity mirrors.

We use the frequency doubled output of a Prometheus (INNOLIGHT GmbH) laser (≈ 20 mW at 532 nm) to provide both the pump and probe beams for our experiment. After optical isolation, the laser output traverses a single mode matching lens. The laser beam is then phase modulated at 30 MHz (NewFocus 4002) prior to splitting the pump (≈ 8.0 mW) and probe (≈ 2.0 mW) beams. The pump and probe beams are then reflected and aligned off 50:50 beam-splitters, before interrogating the ring cavity in opposite directions. A Toptica iodine cell, 12 mm in diameter, 100 mm long, with Brewster angle windows is placed at the cavity waist position. The reflected pump (R_{pump}) and probe (R_{probe}) beams are incident on separate photo-diodes (pd). The RF signal from the pump photodetector is split with one output being demodulated to derive the error signal that is then fed back to the cavity PZT mirror in order to lock the ring cavity on resonance with the laser frequency. The other RF splitter output is also demodulated before being attenuated and subtracted from the independently demodulated RF probe photodetector output. This demodulated pump-probe difference signal can then be used to both detect weak atomic transitions as well as provide an error signal to lock the laser to a hyperfine transition.

Figure 2 shows the resulting signals when the FPI is locked on resonance with the laser and the laser frequency is then scanned across the Doppler broadened R(56)32-0 iodine transition. Traces 2a and 2b show the transmitted power of the pump and probe beams, respectively. The probe transmission exhibits inverted Lamb dips [5] at the hyperfine transition frequencies. The FPI enhances the size of these inverted Lamb dips showing clearly defined features. Trace 2c shows the output of the subtracted error signal. At every hyperfine transition there is a clear error signal due to the differential phase response of the inverted Lamb dips seen only by the probe beam. All traces are recorded with an intra-cavity pump power of approximately 40 mW which leads to substantial power broadening, leaving several hyperfine pairs unresolved. Even so, the subtracted output demonstrates a clear ability to lock the frequency of the laser to any of the well defined error signals. Trace 2d shows a detailed scan of the R(56)32-0 a₁ hyperfine error signal.

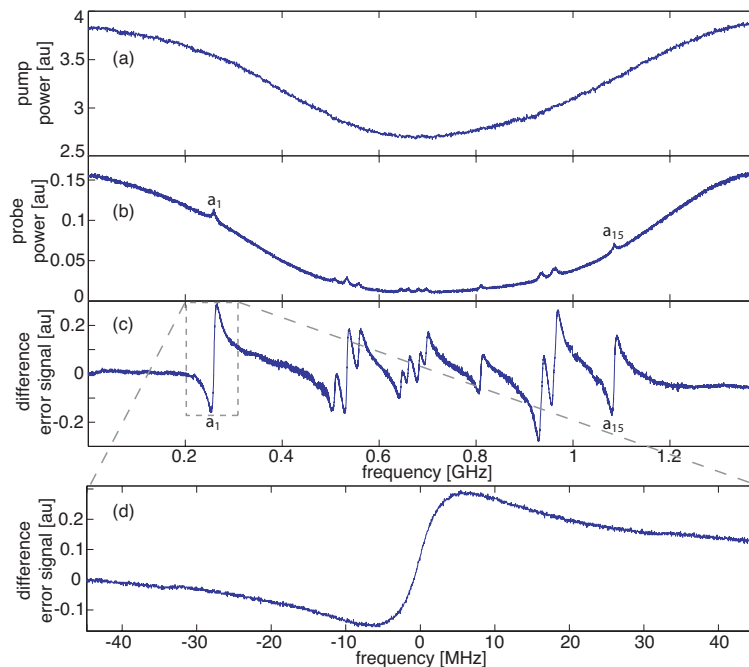


Figure 2. Cavity locked, broad laser frequency scan (≈ 1.4 GHz) across the R(56)32-0 broadened atomic resonance, showing absorption profile for (a) pump power, (b) probe power, (c) associated error signals from demodulated pump-probe difference, and (d) zoom in of R(56)32-0 a₁ hyperfine resonance difference error signal. Traces (c) and (d) are taken with a measurement bandwidth of 1 kHz (figure from [3]).

The noise-canceling effect can be directly observed in the time domain while scanning the laser frequency with the cavity locked (as described above for figure 2) and simultaneously observing the demodulated pump, probe and pump-probe subtraction signals. Figure 3 presents the plots resulting from such a measurement with the cavity locked to the laser frequency while slowly scanning the laser frequency across the R(56)32-0 a₁ hyperfine transition. Noise was deliberately introduced to the cavity by mechanical impulse excitations of the optical bench. Trace 3a shows the demodulated reflected pump signal. As would be expected, with the cavity locked, this is a flat, zero trace and the noise impulses can be seen as spikes in the trace. The demodulated reflected probe signal (shown in figure 3b) has a clear and obvious dispersion shape from the a₁ hyperfine transition (with noise spikes coincident in time with the pump signal).

This shows that the pump is saturating the R(56)32-0 iodine transition, allowing the probe to interact with the hyperfine transitions. This was described and can also be seen in figures 2a and 2b. With the demodulated reflected probe signal we now have a cavity-enhanced measure of the a1 hyperfine dispersion signal. As can be seen, this signal is suitable for use as an error signal in order to feed back and stabilise the laser frequency. However, it can also be seen that a direct consequence of the cavity-enhancement is the coupling of any cavity mechanical noise into the signal. After subtracting the signals shown in figures 3a and 3b via a differential amplifier, we obtain the signal, $\Sigma-$, shown in figure 3c which is clearly free from the noise seen in both the pump and probe signals alone.

Since the reflected probe signal changes in both amplitude and phase as the laser frequency scans across the hyperfine transition, the subtraction can only be optimised for one particular laser frequency (or, equivalently, at one point on the hyperfine transition). In practical terms, this optimisation is carried out with the laser frequency at the centre of the hyperfine transition which we wish to use as our frequency reference. This ensures that we have the best noise-canceling performance from our system at the required laser frequency. The noise-canceling effectiveness of this subtraction technique can be analysed in more detail in the frequency domain by looking at noise spectral densities of the pump, probe and difference signals (see [3]).

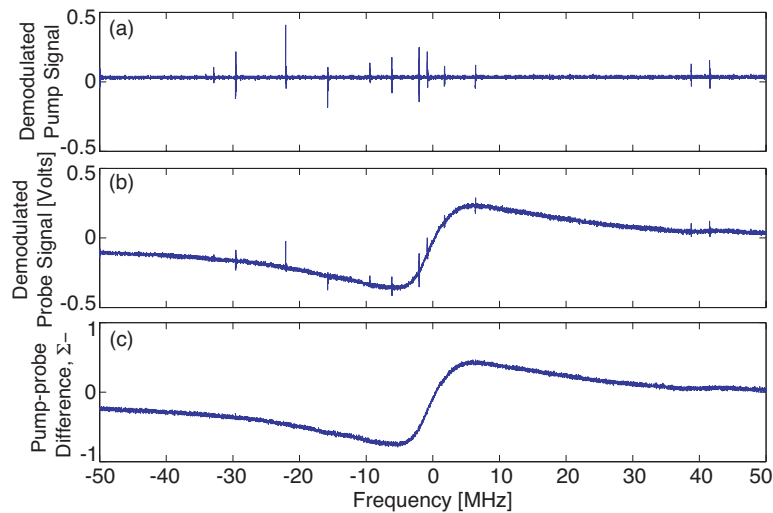


Figure 3. Demodulated reflected (a) pump and (b) probe signals with deliberate mechanical noise spikes. Trace (c) shows the noise-canceling effect on the pump-probe difference signal.

2.2. Laser frequency stabilisation

Two experimental systems identical to that shown in figure 1 were set up, each in front of its own laser (identical Prometheus lasers) on the same optical bench. The pump-probe differential hyperfine error signal (as shown in figures 2d and 3c) from each system was fed back via a laser frequency servo to both the Nd:YAG laser crystal temperature and PZT actuators for each laser. This stabilised the frequency of each laser to the a1 hyperfine frequency reference. The frequency servo had a unity gain frequency of approximately 30 kHz.

The two 1064 nm outputs, one from each laser, were then interfered on a 50:50 beamsplitter with the resulting heterodyne beat signal detected by an InGaAs photodetector and monitored using a frequency counter (Stanford Research Systems SR620 Universal Time Interval Counter), with the data being logged using LabView on a PC. The maximum sampling frequency was 10 Hz.

Initial stability data has been taken, with some analysis presented below. Figure 4 shows the heterodyne beat frequency between the two lasers plotted as a time series for 1000 s of data with the frequency normalised to the average beat frequency for the time interval. This gives an indication of the frequency fluctuations (or deviation) over time. The normalised free-running laser frequency fluctuations are shown in figure 4 as trace (i). It can be seen that there is a relative frequency drift of approximately 12 MHz over 1000 s. Traces 4(ii) and 4(iii) show the same plot of the frequency stabilised heterodyne beat with the frequency axis of trace 4(iii) being 100 times that of traces 4(i) and 4(ii). From trace 4(iii) it can be seen that there is a relative frequency drift of approximately 30 kHz over 1000 s. From these numbers it can be seen that the relative frequency stability is improved by a factor of 400 over a 1000 s period.

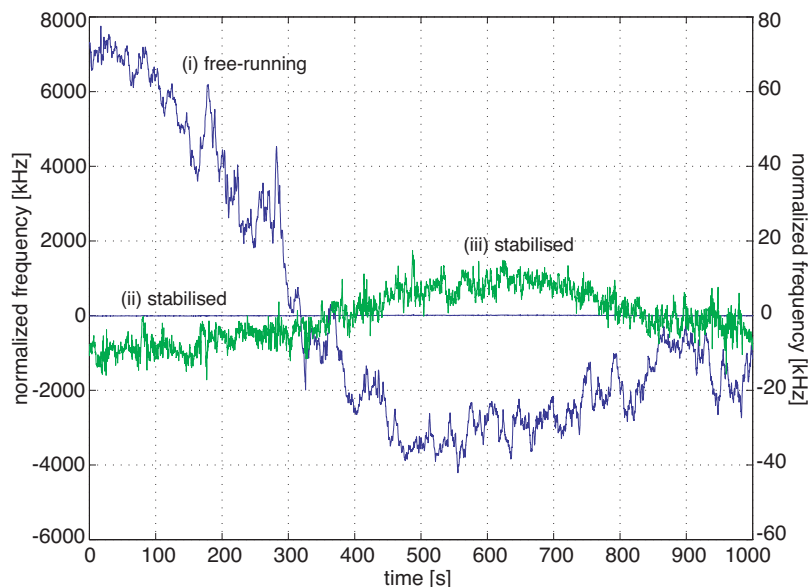


Figure 4. Time series of frequency fluctuations showing the normalised heterodyne beat frequency fluctuations for: (i) both lasers free-running, (ii) both lasers stabilised, and (iii) trace (ii) again (both lasers stabilised) with the vertical (frequency) axis zoomed 100 \times (the scale is given on the right side of the plot).

The normalised Allan deviation (or root Allan variance) [6] has been calculated for both lasers free-running and both lasers stabilised. This is presented in figure 5, where trace 5(i) is the free-running and 5(ii) is the stabilised Allan deviation. For an integration time of 0.1s we have achieved a normalised root Allan variance of 2×10^{-12} , with 3×10^{-11} at an integration time of 400 s. While these initial results are a few orders of magnitude away from more mature and leading experimental techniques (such as [7, 8]), the results show that our technique is already competitive with other spectroscopic techniques in the current literature, for example, see [9]. This cavity-enhanced technique has a shot-noise limited sensitivity surpassing non-cavity based techniques. Further work needs to be carried out in order to reduce other noise sources/floors and achieve shot-noise-limited measurements.

3. Conclusions

Initial laser frequency stabilisation results have been obtained employing a new noise-canceling, cavity-enhanced spectroscopic technique. We have demonstrated the capability of our technique in giving a cavity-enhanced, noise-free, sub-Doppler spectroscopic measurement. In this case

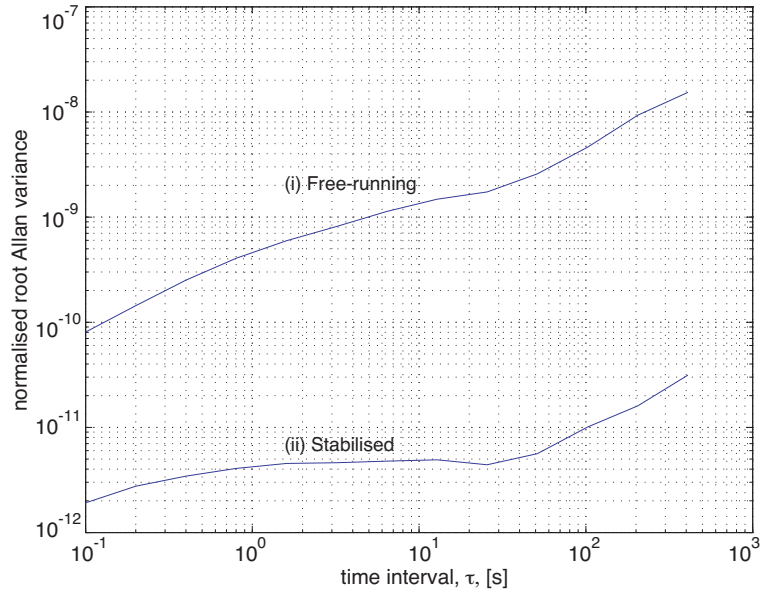


Figure 5. Allan deviation plots for (i) both lasers free-running and (ii) both lasers locked to the R(56)32-0 a1 iodine hyperfine transition.

we use this signal as a frequency reference error signal for feeding back and stabilising the fundamental laser frequency. We have improved the free-running laser frequency stability by over two orders of magnitude. At 0.1s and 400s integration times we have achieved a normalised root Allan variance of 2×10^{-12} and 3×10^{-11} , respectively. Further data analysis and experimental noise-hunting is being carried out in order to further improve the frequency stability.

Acknowledgments

This research was completed at the Centre for Gravitational Physics, a member of the Australian Consortium for Interferometric Gravitational Astronomy, with partial support from the Australian Research Council.

- [1] P. Bender and K. Danzmann and the LISA Study Team, *Laser Interferometer Space Antenna for the detection and observation of gravitational waves: Pre-Phase A Report 2nd Edition*, Max-Planck-Institut für Quantenoptik, Garching, Germany, **MPQ233**, (1998).
- [2] P. Cerez, A. Brillat and C. N. Man-Pichot, *He-Ne lasers stabilised by saturation absorption in iodine at 612 nm*, IEEE Trans. Instrum. Meas., **29**, 352-354, (1980).
- [3] G. de Vine, J. Close, D. E. McClelland and M. B. Gray, *Pump-probe differencing technique for cavity-enhanced, noise-canceling saturation laser spectroscopy*, Opt. Lett., **30**, 10 (2005).
- [4] R. W. P. Drever, J. L. Hall, F. V. Kowalski, J. Hough, G. M. Ford, A. J. Munley and H. Ward, *Laser phase and frequency stabilization using an optical resonator*, Appl. Phys. B, **31**, 97, (1983).
- [5] W. E. Lamb, *Theory of an optical maser*, Phys. Rev., **134**, A1429, (1964).
- [6] D. W. Allan, *Statistics of atomic frequency standards*, Proc. IEEE, **54**, 221230, (1966).
- [7] Jun Ye, Lennart Robertsson, Susanne Picard, Long-Sheng Ma, and John L. Hall, *Absolute Frequency Atlas of Molecular Lines at 532 nm*, IEEE Trans. Instrum. Meas., **48**, 544-549, (1999).
- [8] K. Nyholm, M. Merimaa, T. Ahola, and A. Lassila *Frequency Stabilization of a Diode-Pumped Nd:Yag Laser at 532 nm to Iodine by Using Third-Harmonic Technique*, IEEE Trans. Instrum. Meas., **52**, 284-287, (2003).
- [9] P. Burdack, M. Trbs, M. Hunnekuhl, C. Fallnich, and I. Freitag, *Modulation-free sub-Doppler laser frequency stabilization to molecular iodine with a common-path, two-color interferometer*, Opt. Express, **12**, 644-650, (2004).